

Spectral-Directional Emittance of Thermally Oxidized 316 Stainless Steel

P. D. Jones^{1,2} and E. Nisipeanu¹

Received October 12, 1995

The spectral-directional emittance of thermally oxidized stainless steel is measured for angles from normal to grazing, wavelengths between 2 and 10 μm , and temperatures between 773 and 973 K. The oxide is grown by holding the steel substrate at a high temperature over a long period while exposed to normal atmospheric conditions, until the measured emissive power of the surface achieves an asymptotic level. It is found that the emittance decreases with angle away from the surface normal at the lower end of the measured spectral range and increases with angle at the higher end. The emittance decreases with wavelength, although there is evidence of a peak near 2 μm . The variation with temperature within the measured range is insignificant. Overall higher values for the oxidized steel are measured than those reported in previous work.

KEY WORDS: directional radiative surface properties; emittance; optical properties; oxides; spectral radiative surface properties; stainless steel.

1. INTRODUCTION

Radiation heat transfer methods which can conveniently account for directional as well as spectral variations in surface properties are becoming more tractable for industrial use [1], resulting in a need for spectral-directional radiative surface properties data. At the elevated temperatures common when radiation is a significant heat transfer mode, stainless steel is a commonly used material. At elevated temperatures, stainless steel in atmospheric air develops a light thermal oxide, typically Cr_2O_3 . This oxide grows over time to a limiting thickness, which is achieved more quickly at higher temperatures. The object of this paper is therefore the presentation

¹ Mechanical Engineering Department, Auburn University, Auburn, Alabama 36849-5341, U.S.A.

² To whom correspondence should be addressed.

of measurements of the spectral-directional emittance of type 316 stainless steel which has been allowed to oxidize thermally by holding it at an elevated temperature for an extended time. The goal of such work is the development of thermophysical property data for use with advanced radiation heat transfer computational methods in the analysis of commonly applied materials.

An approach for determining the spectral-normal emittance of oxidized metals as a function of the complex indices of refraction of both the metal and the oxide is offered by Brannon and Goldstein [2]. For instance, Karlsson et al. [3] grew a film of Cr_2O_3 on a glass substrate, derived the index of refraction of the oxide from reflectance measurements in the normal direction, and combined this with reported index data for stainless steel to predict the emissive performance of a thin oxide layer (80 nm) on a stainless-steel substrate. Comparison to measurements for a similar thin oxide layer on a chromium substrate shows qualitative agreement. Brannon and Goldstein themselves studied thicker oxide layers ($1\ \mu\text{m}$ and higher) on aluminum and copper substrates, finding that their method underpredicts emittance compared to measurements on complete oxide/metal systems. Since this analytical method is tractable only for the normal direction, and has not been proven to be uniformly accurate even in that direction (especially at oxide thicknesses of the order of those grown in the present work), it remains necessary to make experimental measurements to determine the radiative properties of fully oxidized stainless steel.

Experimental studies of the emittance of oxidized stainless steel are presented by Demont et al. [4] and by Huetz-Aubert and Sacadura [5]. Both of these works concern type 304 stainless-steel samples, oxidized for 2 h at 573, 673, and 773 K. (The emissivities of plain 304 and 316 stainless steels are demonstrated to be very similar by Demont et al.) Results are presented only for the normal direction. Measurements cover the visible range of the spectrum and the infrared range out to $11\ \mu\text{m}$. In the infrared range between 1 and $11\ \mu\text{m}$ (which concerns the present work), both studies conclude that there is relatively little difference between the normal emittance of plain stainless steel and the normal emittance of oxidized stainless steel (results show about a 20% difference), compared to the larger difference found in the visible range. Demont et al. present further data on the difference in emittance of their 773 K oxidized sample measured at both 300 and 773 K and conclude that there is little temperature effect in the emittance of oxidized stainless steel.

In the present work, full directional distributions of the emittance of oxidized 316 stainless steel are measured over the spectral range from 2 to $10\ \mu\text{m}$, as opposed to only the normal direction. The sample is allowed to

oxidize fully over a period of several days and its approach to a steady level of emitted intensity is monitored, in order to ensure that a definable level of oxidation has been achieved. Emittance measurements are taken over a range of temperatures to confirm whether or not this parameter plays a role. The intent of this work is to provide emittance data for use in radiation heat transfer studies which can account for the full variation of emittance with wavelength, direction, and temperature.

2. APPARATUS

Surface emittance is determined using an apparatus for the measurement of radiative intensity (or, more precisely, measurement of radiative

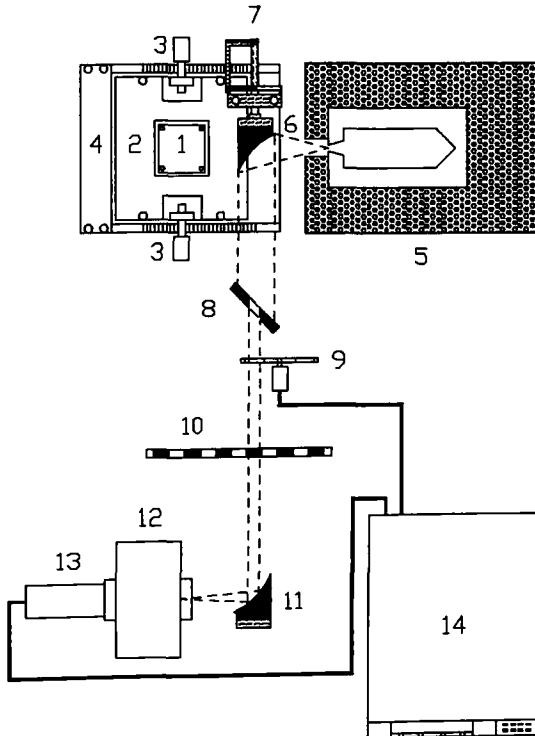


Fig. 1. Radiation intensity measurement system: plan view. System components: (1) sample; (2) sample holder; (3) trunnions; (4) slotted arc rack; (5) blackbody; (6) collecting reflector; (7) reflector rotation mechanism; (8) trimming plate; (9) chopper; (10) filter rack; (11) refocussing reflector; (12) monochromator; (13) detector; (14) radiometer.

flux within a finite cell of solid angle and band of wavelength), which is shown in Fig. 1 (plan view). This apparatus is described more fully in Ref. 6. Briefly, with reference to Fig. 1, radiative intensity exiting a sample surface (1) within a finite solid angle is intercepted by a parabolic collection mirror (6), turned, and collimated. The collimated beam is trimmed by an aperture (8), which is angled so that the trimmed intensity cannot be reincident on the sample surface. The beam is chopped (9) in order to create a modulated signal and filtered (10) to block wavelength overtones. The collimated beam is refocused (11) into a $\frac{1}{8}$ -m grating monochromator (12), and the flux within the resulting wavelength band is incident on a detector (13; electrically polarized lithium tantalate crystalline chip). Detector interpretation and chopper control are accomplished by a phase-locked amplifying radiometer (Oriel Merlin). The optical path length is 1.1 m, all in atmospheric air.

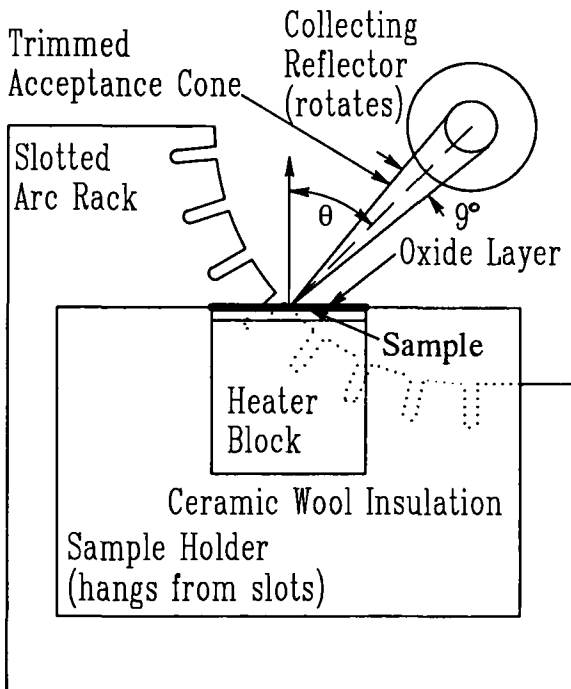


Fig. 2. Arrangement for varying intensity measurement direction relative to the surface normal: elevation viewed from axis of optical path.

The radiometer reading is calibrated by using a rotating mechanism (7) to turn the mirror (6) to face a radiating cavity blackbody (5), which is machined into 152-mm-diameter copper stock, has an automatically controlled wall temperature, and is packed in insulation blanket 76 mm thick. The sample surface is attached to a copper heater block (76-mm cube) with automatically controlled temperature. The heater block and sample are packed in insulation blanket up to the plane of the sample surface (nothing protrudes beyond the sample surface). The heater, sample, and insulation are contained in a box-shaped casing (2). The casing is suspended by trunnions (3) from a fixed circular arc rack (4), as shown in elevation in Fig. 2. By rotating the mirror (6) and moving the casing (2) to the appropriate position in the rack (4), the polar angle (relative to the surface normal) of the intensity accepted by the measurement system is varied between 0° (normal) and 84° (grazing; the width of the accepted solid angle does not allow $\theta > 84^\circ$). The acceptance solid angle of the intensity measurement system optical path is 0.020 sr (maximum polar variation, 9°), while the monochromator passes a wavelength band that varies between $0.026 \mu\text{m}$ in width at a wavelength of $1.5 \mu\text{m}$ and $0.16 \mu\text{m}$ in width at $10 \mu\text{m}$.

3. MEASUREMENT PROCEDURE

The intensity measurement system is calibrated in advance using the blackbody, measuring the correlation of measurement signal with blackbody intensity as a function of temperature and wavelength. Repeated measurements of this correlation demonstrate a variance of 1 to 2% for most readings and as high as 3% for some. Higher variances occur at lower temperatures and at both very high and very low wavelengths, where the signal strength is lower. For this reason, measurements are limited (in the present application) to temperatures above approximately 773 K, and wavelengths between 2 and $10 \mu\text{m}$. The highest sample surface temperature which the apparatus is designed to maintain is 973 K.

A sample of type 316 stainless steel, $76 \times 76 \times 6$ mm thick, was milled to a No. 8 lathe finish (polished smooth, but not mirror-like, with small scratches and imperfections plainly visible) and thoroughly cleaned to remove foreign films and particles. The sample was attached to the heater block. A thermocouple probe was extended through the heater block and into the sample, with its tip just below the sample surface (conjugate combined mode heat transfer analysis shows a predictable difference between measurement point and actual surface temperature of 1 to 2 K). The sample was heated to 973 K and held at this temperature for over 120 h while the measured normal intensity was monitored. This intensity reached asymptotic levels well before the end of the heating period, indicating that

oxide layer growth on the sample was no longer altering the surface emittance. Complete spectra of surface emission were measured by adjusting the monochromator grating angle and stepping through the range of prefilters. The directional range was covered by jointly adjusting the collection mirror angle and the sample casing position. With complete spectra and directional range measurements, the temperature was decreased in 100-K increments to 773 K. Measurements were compared to calibration measurements taken previously to determine the surface emittance. (The blackbody is kept cool during sample measurements, as are all other surfaces in view of the sample surface, in order to limit reflective contributions to the measured signals.)

X-ray diffraction and scanning electron microscope analyses were applied to the sample surface and to scrapings from the surface to verify the oxide composition. The results of these analyses are not inconsistent with the expectation that Cr_2O_3 would be grown. Further SEM study of a section of the sample cut out by electron discharge machining indicates that the oxide layer is between 2 and 3 μm thick.

4. DATA REDUCTION

An intensity measurement system calibration factor C is determined according to

$$C(\lambda, T_c) = \frac{1}{R_c(\lambda, \theta, T_c)} \left[\int_{\lambda - \delta\lambda/2}^{\lambda + \delta\lambda/2} I_{\text{lb}}(T_c) d\lambda \right] \delta\Omega \quad (1)$$

where R_c is the radiometer measurement taken with the calibration blackbody set at temperature T_c , $\delta\lambda$ is a wavelength interval about wavelength λ , θ is a polar angle relative to the surface normal, I_{lb} is the blackbody intensity, and $\delta\Omega$ is a finite solid angle. The spectral-directional emittance ε is determined by

$$\varepsilon_{\lambda, \theta}(T_s) = \frac{R_s(\lambda, \theta, T_s) C(\lambda, T_s)}{\left[\int_{\lambda - \delta\lambda/2}^{\lambda + \delta\lambda/2} I_{\text{lb}}(T_s) d\lambda \right] \delta\Omega} \quad (2)$$

where R_s is the radiometer measurement taken from the sample surface, and T_s is the sample surface temperature. The measurement solid angle $\delta\Omega$ about θ and the measurement wavelength band $\delta\lambda$ about λ are held fixed between R_c and R_s . As long as T_s and T_c do not differ, the data reduction system of Eqs. (1) and (2) amounts to simply the ratio of R_s to R_c .

5. UNCERTAINTY ANALYSIS

Combining Eqs. (1) and (2), the uncertainty in the spectral-directional emittance may be stated

$$u_{\varepsilon}^2 = \left(\frac{\partial \varepsilon}{\partial R_c} u_{R_c} \right)^2 + \left(\frac{\partial \varepsilon}{\partial R_c} u_{R_c} \right)^2 + \left(\frac{\partial \varepsilon}{\partial T_c} u_{T_c} \right)^2 + \left(\frac{\partial \varepsilon}{\partial T_s} u_{T_s} \right)^2 \quad (3)$$

where u is the uncertainty of its subscript and $\delta\Omega$ and $\delta\lambda$ are considered to be perfectly repeatable. Considering that as $T_c \approx T_s$, $I_{\lambda b}(T_c) \approx I_{\lambda b}(T_s)$, this may be reduced to

$$u_{\varepsilon}^2 = (1 + \varepsilon^2) \left[t_{5,90} \left(\frac{S_{R_c}}{R_c} \right) \right]^2 + \left(\frac{4\varepsilon}{T_s} \right)^2 (u_{T_c}^2 + u_{T_s}^2) \quad (4)$$

for six complete calibration spectra and a 90% confidence level, where S is a sample deviation and t is a Student t distribution parameter. For the range of data presented here, the uncertainty in emittance is dominated by the radiometer measurement uncertainty. Other sources of uncertainty, including the effects of incidence from background radiation, are shown to be insignificant. For these data, the uncertainty in spectral-directional emittance varies between 2 and 3% of the emittance value, with some uncertainties (typically for lower temperatures and wavelengths at the high and low extremes) as high as 4 or 5%.

6. RESULTS AND DISCUSSION

Figure 3 shows emittance data as a function of direction (polar angle) at various wavelengths for fully oxidized type 316 stainless steel. These data were measured at a surface temperature of 773 K. Data taken at 873 and 973 K are similar in functional form and vary very slightly in magnitude (drifting very slightly up with temperature), though this variation is well within the experimental uncertainty. At shorter wavelengths ($2 \leq \lambda \leq 6 \mu\text{m}$), the emittance of the steel with a 2 to 3- μm -thick layer of Cr_2O_3 is in the range of 0.4 to 0.5, with a directional behavior somewhat like a dielectric (monotonic decrease with increasing polar angle). This is because the oxide thickness is of the order of the wavelength, and the dielectric oxide has a significant influence on the behavior of the oxide/steel system. At longer wavelengths, the emittance is lower, in the range of 0.2 to 0.3, and has a more metallic directional character (a slight increase with polar angle up to a grazing angle, then a sharp decrease). This correlates with the reduced effect of the thinner (relative to wavelength) oxide film.

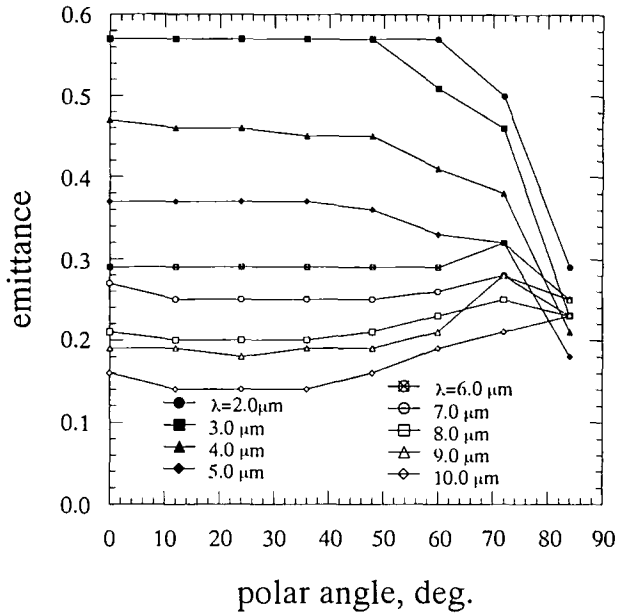


Fig. 3. Measured spectral-directional emittance of fully oxidized type 316 stainless steel at various wavelengths as a function of direction (surface temperature, 773 K).

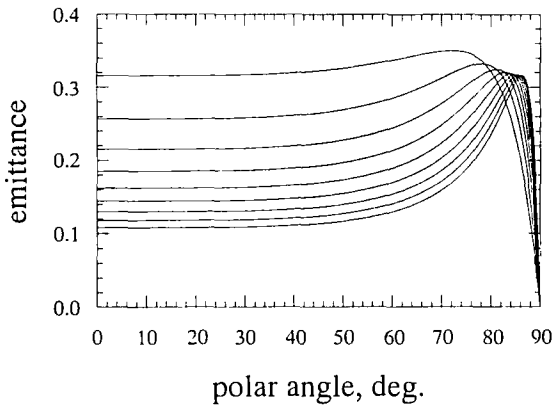


Fig. 4. Calculated spectral-directional emittance of plain type 316 stainless steel at various wavelengths (same as Fig. 3; highest emittance corresponds to 2 μm) as a function of direction.

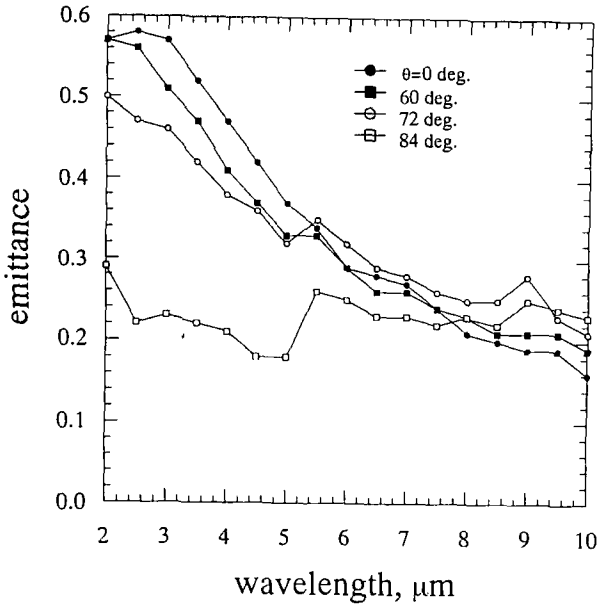


Fig. 5. Measured spectral-directional emittance of fully oxidized type 316 stainless steel at various directions as a function of wavelength (surface temperatures 773 K).

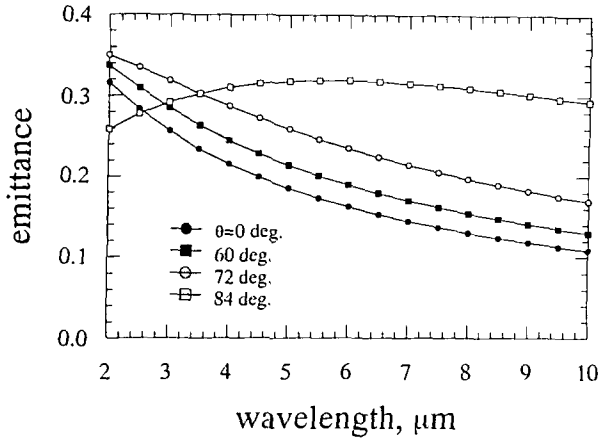


Fig. 6. Calculated spectral-directional emittance of plain type 316 stainless steel at various directions as a function of wavelength.

The measured emittance is significantly higher than that for plain type 316 stainless steel. Heinisch et al. [7] measured the spectral-directional emittance of 316 at 773 K using a direct-measurement, polarized-radiation, double-beam technique. The effective complex index of refraction as a function of wavelength was identified from these data. Comparison to the predictions of the Fresnel equations [8] using this index was found to be excellent. In Fig. 4, the index of refraction data of Heinisch et al. for the plain steel are applied to the Fresnel equations. Comparison of Figs. 3 and 4 shows that the oxide layer has a very significant effect on emittance, affecting both magnitude and directional behavior. The effect on magnitude is of the order of 80% at lower wavelengths and about 50% at higher wavelengths. This is contrary to the finding of Demont et al. [4] that oxidation increases the emittance magnitude by only about 20%. It is probable that the steel samples in the earlier work were not allowed enough time to oxidize fully.

Figure 5 shows the spectral behavior of emittance of the oxidized stainless steel. The spectrum of the normal emittance is similar in appearance to that shown by Demont et al. [4], although at a higher magnitude. The normal emittance decreases across the measured spectral

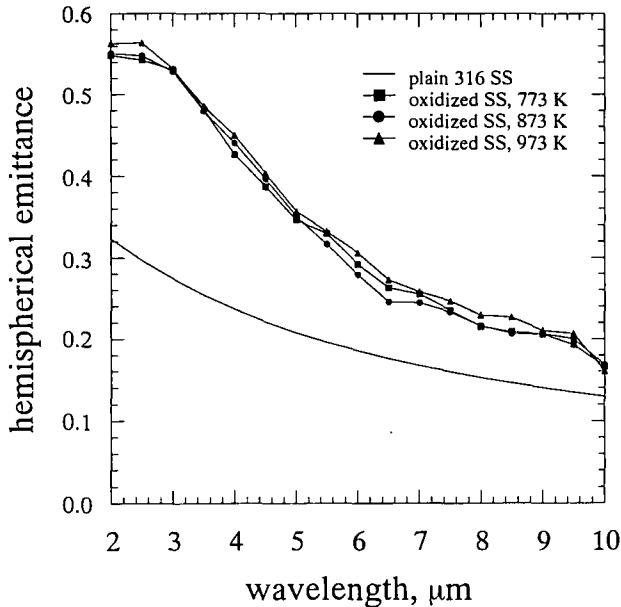


Fig. 7. Measured spectral-hemispherical emittance of fully oxidized type 316 stainless steel at various temperatures as a function of wavelength.

range from about 0.57 at $2\ \mu\text{m}$ to about 0.18 at $10\ \mu\text{m}$. Data for polar angles $0 < \theta < 60^\circ$ are not shown in the interest of clarity and lie entirely within the bounds defined by the $\theta = 0$ and the $\theta = 60^\circ$ lines. For $\theta > 60^\circ$, the spectral variation decreases, and at a grazing angle $\theta = 84^\circ$, the emittance is relatively gray over the measured range of wavelength. The data in Fig. 5 were measured at a surface temperature of 773 K. Data taken at 873 and 973 K are very similar. Note that the oxide layer is too thick for the quarter-wavelength interference minimum to be observed in the measured wavelength range (at $\lambda = 4nd$, and considering Karlsson and co-workers [3] result of $n \approx 2.1$ for Cr_2O_3).

Figure 6 shows the results of Fresnel equation calculations using the complex index of refraction of Heinisch et al. [7] for plain (unoxidized) type 316 stainless steel. The trend of a general decrease with increasing wavelength at nongrazing angles and relatively gray behavior at grazing angles is in agreement with the oxidized surface results, although the emittance of the oxidized surface is much higher than the emittance of the plain steel.

The directional emittance data were integrated to yield spectral-hemispherical emittances. The quadrature suggested in Ref. 9 was employed. The results are shown in Fig. 7 for surface temperatures of 773, 873, and 973 K. The spectral-hemispherical emittance of plain type 316 stainless steel is also shown. As demonstrated in Fig. 7, there is very little variation in the emittance of the oxidized surface with temperature, although a very slight increase with increasing temperature may be inferred. The emittance of the oxidized surface is 50 to 80% higher than the emittance of the plain steel, and not the 20% suggested by Demont et al. [4]. The measured emittance seems to demonstrate a peak around $\lambda = 2\ \mu\text{m}$, as demonstrated by Fig. 7 and by measurements (not shown) at $\lambda = 1.5\ \mu\text{m}$ for 873 and 973 K. Demont et al. show a similar peak, though with a higher magnitude ($\epsilon \sim 0.9$) and at a shorter wavelength ($\lambda \sim 0.4\ \mu\text{m}$). It may be that increasing the thickness of the oxidation layer causes a shift in the emittance spectrum toward higher wavelengths, coupled to a decrease in the peak magnitude of that spectrum. Further research on this point seems warranted.

7. CONCLUSIONS

The spectral-directional emittance of type 316 stainless steel, fully oxidized with a 2- to 3- μm -thick Cr_2O_3 layer, is derived from measurements of the radiative intensity leaving the surface of an oxidized steel plate. The oxide layer is grown under room atmospheric conditions to its limiting thickness by holding it at elevated temperatures over long heating times and is not dressed or polished in any way. Emittance data for this material show

values significantly higher than the emittance of the plain (unoxidized) steel. This conclusion is at odds with the results of previously reported measurements, although it is possible that in the earlier work a limiting oxide layer thickness was not achieved. Directional behavior shows a characteristic dielectric form for wavelengths of the order of $2\ \mu\text{m}$ and a metallic form for wavelengths of the order of $10\ \mu\text{m}$. Spectral behavior shows a decreasing monotonic variation with wavelength between 2 and $10\ \mu\text{m}$ at nongrazing angles and near-gray behavior at grazing angles. Variation with temperature over a range from 773 to 973 K is insignificantly slight. A peak in the emittance is indicated near a wavelength of $2\ \mu\text{m}$, whereas the earlier work reported a peak near $0.4\ \mu\text{m}$. Possible shift of this peak with growth of the oxide layer might be worth investigation.

ACKNOWLEDGMENTS

Funding for this work was provided by the National Science Foundation, under Grant CTS-9209926, whose support is gratefully acknowledged. Prof. Jeffrey W. Fergus and Prof. William F. Gale graciously provided X-ray diffraction and scanning electron microscope expertise to help characterize the oxide.

REFERENCES

1. W. A. Fiveland and J. P. Jessee, *J. Thermophys. Heat Trans.* **9**:47 (1995).
2. R. R. Brannon and R. J. Goldstein, *J. Heat Trans.* **92**:257 (1970).
3. B. Karlsson, C. G. Ribbing, A. Roos, E. Valkonen, and T. Karlsson, *Phys. Scrip.* **25**:826 (1982).
4. Ph. Demont, H. T. Nguyen, and J. F. Sacadura, *J. Physique* **42**(C1):161 (1981).
5. M. Huetz-Aubert and J. F. Sacadura, *Rev. Phys. Appl.* **17**:251 (1982).
6. P. D. Jones, D. E. Dorai-Raj, and D. G. McLeod, AIAA 95-3521 (1995).
7. B. Heinisch, P. Quinto-Diez, and J. F. Sacadura, *Proc. 7th Int. Heat Trans.* **4**:509 (1982).
8. R. Siegel and J. R. Howell, *Thermal Radiation Heat Transfer* (Hemisphere, Washington, DC, 1992), pp. 112–130.
9. P. D. Jones, D. G. McLeod, and D. E. Dorai-Raj, *J. Heat Trans.* **118**:94 (1996).